GSA Data Repository 2018008

Boiling induced formation of colloidal gold in black smoker hydrothermal fluids

Amy Gartman[1], Mark Hannington[2,3], John W. Jamieson[4], Ben Peterkin[4], Dieter Garbe-Schönberg[5], Alyssa J. Findlay[6*], Sebastian Fuchs[2], Tom Kwasnitschka[2]

[1.] *US Geological Survey, PCMSC, 2885 Mission St., Santa Cruz, California, 95060, USA*

[2.] *GEOMAR – Helmholtz Centre for Ocean Research Kiel, 1-3 Wischhofstr., 24148 Kiel, Germany*

[3.] *Department of Earth Sciences, University of Ottawa, Ottawa ON Canada, K1N 6N5*

[4.] *Department of Earth Sciences, Memorial University of Newfoundland St. John's, NL, Canada A1B 3X5*

[5.] *Institute of Geosciences, Kiel University, Ludewig-Meyn-Strasse 10, 24118 Kiel, Germany*

[6.] *Department of Geological and Environmental Sciences, Ben-Gurion University of the Negev, Beer Sheva, Israel*

[*] *Current Address: Center for Geomicrobiology, Department of Biological Sciences, Aarhus University, Aarhus C, Denmark*

1. Sampling Locations

All samples were collected from vents occupying a 500-m diameter explosion crater on the south flank of the Niua South volcanic cone (Fig. S1, Table S1).

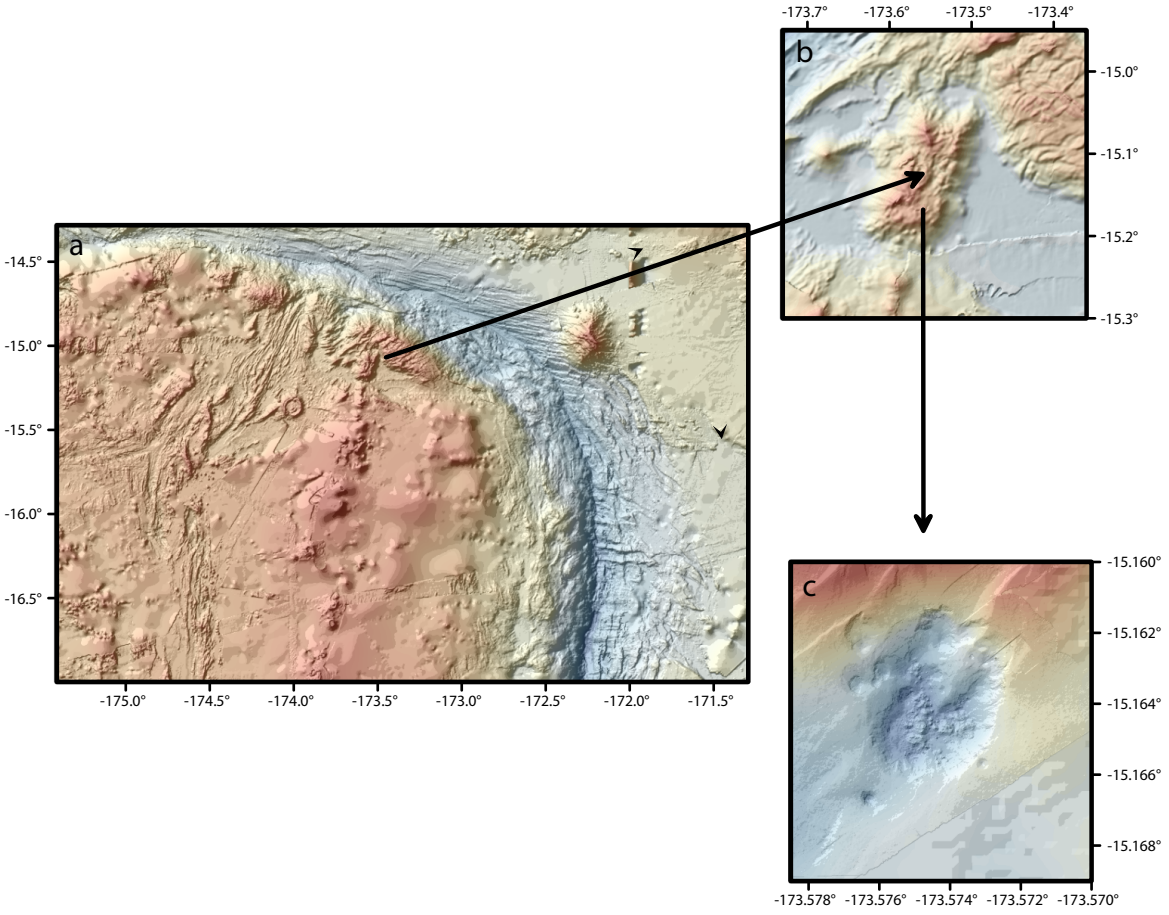

Fig. S1. Location of the Niua Volcano at the northern termination of the Tonga volcanic arc (a). Niua is a large, 20-km long volcanic complex (b) comprising two volcanic cones (Niua North and Niua South). The Niua South hydrothermal field (c) occupies a 500-m diameter explosion crater on the southeast flank of the cone. Unpublished bathymetric data provided by Nautilus Minerals, Inc. and GEOMAR. Niua South first sampled by Resing et al., 2012.

	Location	Location	Sample (sulfide chimney)	Sample (fluid)	Depth (m)	T (°C)	pH	Mg (mM)	% seawater	Au (nM)	AVS +CRS (mM)	Au (ppb)
Boiling	-15.16316167	-173.5746983	D1918-R4	1918 blue	1164	325	3.14	4.00	8	3.08	1.28	5590
				1918 yellow	1163	325	3.84	14.98	28	3.68	0.39	
Focused flow	-15.16286667	-173.5746367	N/A	1918 orange	1155	302	5.98	38.27	73	3.05	0.02	N/A
				1918 red	1155	302	4.12	23.58	45	2.91	0.80	
	-15.16476833	-173.5736017	D1919-R6 A,B	1919 yellow	1151	300	3.36	3.44	7	1.61	0.86	11400, 3640
				1919 green	1151	300	4.73	27.96	53	2.03	0.34	
	-15.16466167	-173.5742267	D1919-R4	1919 grey	1155	316	3.62	12.11	23	3.11	1.08	6550
				1919 red	1155	316	4.43	22.76	43	5.38	0.57	
	-15.16550167	-173.5739017	N/A	1920 blue	1146	278	4.57	21.09	40	1.60	0.39	N/A
Diffuse flow	-15.16489333	- 173.5729333	D1920-R15	1920 orange	1142	250	4.14	31.36	60	26.73	0.26	>30000

Table S1- the locations and relevant chemical data for fluids, as well as gold concentrations (ppb, last column) for corresponding sulfide chimney samples. Details of sample measurements are included in the subsequent text. Percent seawater is derived from the concentration of magnesium in the sample and assuming a seawater concentration of 52.7 mM Mg, and an end member hydrothermal fluid concentration of 0 mM Mg.

2. Fluid Sampling and Analysis

Samples were collected by the remotely operated vehicle (ROV) ROPOS, using titanium major samplers (750 mL). Prior to sampling, the temperature of the orifice was measured using the high-temperature probe on the ROV. Four of the six sites were sampled in duplicate. Sampling

of the boiling vent resulted in the precipitation of a black tarnish on the sampler snorkel (Fig. S2), the tarnish was mainly composed of metal sulfides.

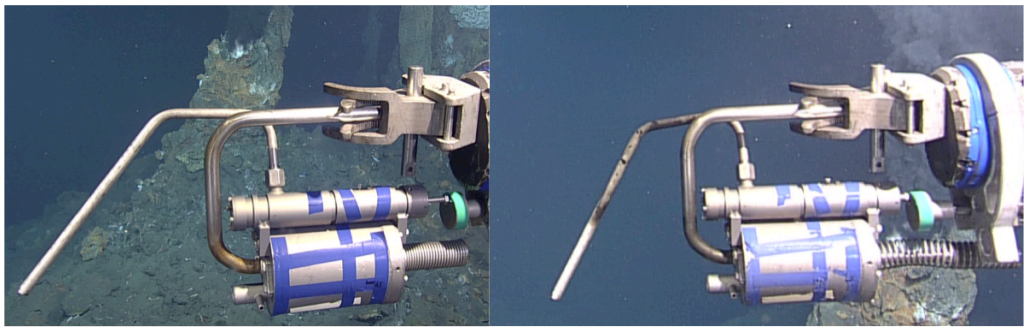

Fig. S2- Photographs pre (left) and post (right) sampling of the boiling vent, demonstrating the black tarnish observed to precipitate on the snorkel of the boiling sample. Similar tarnish was not observed after sampling any of the other vents. The tarnish was mainly composed of metal sulfides, and also contained abundant gold particles.

Samples were processed immediately upon shipboard recovery, 1-8 hours after sample collection, at which point the temperature and pH of the fluids within the samplers was also recorded. Shipboard temperatures were between 20 and 25°C. Separate aliquots were taken for measurement of major and trace elements, acid volatile sulfide/chromium reducible sulfur (AVS/CRS), and particle analysis. Whole fluids were used for both major element and trace element analysis. For major elements, samples were acidified with HCl to below pH 1 and immediately frozen at -20°C. Subsamples for trace elements were frozen whole without amendment. Samples for AVS/CRS were fixed with 1 M NaOH and 0.1 M zinc acetate for acid and also frozen at -20°C. Subsamples for particle analysis were centrifuged shipboard, according to the method described by Gartman et al. (2014).

68 Samples for major elements were further leached upon return to shore with nitric acid for at least
69 48 hours and then filtered through a 0.2 μm Puradisc Nylon filter, diluted 100 fold in 2% HNO_3
70 and analyzed on a Perkin Elmer NexION 300Q at the U.S. Geological Survey, Menlo Park, CA.
71 Be 9, Ge 74 and Tl 205 were run as internal standards. Analytical precision determined by repeat
72 analyses is better than 5%. Data for Mg are reported in this study; the other major elements will
73 be reported elsewhere. The trace elements, including gold, were measured on whole samples
74 (unfiltered) that were acidified in the laboratory with subboiled HNO_3. Insoluble precipitates in
75 unfiltered aliquots were centrifuged and pressure-digested over night at 160°C in PFA vials
76 (Savillex) using a multistep mixed acid procedure with HF-aqua regia. The digested liquids were
77 analyzed with both matrix-matched calibration and standard addition by high resolution ICP-SF-
78 MS (Thermo Scientific Element XR) in the ICP-MS Laboratory of the Institute of Geosciences,
79 Kiel University, following the approach and methods described in Garbe-Schönberg (1993) and
80 Koschinsky et al. (2008). Analytical precision determined by repeat analyses of fluid samples is
81 <1-7% RSD. Limits of quantification (L.O.Q.) for each element, based on the whole procedure
82 are determined by repeat analysis of blanks on each instrument and monitored by control
83 samples and duplicates. The accuracy of the results was assessed by analyzing NASS-5
84 Reference Seawater (NRCC National Research Council of Canada), IAPSO Standard Seawater
85 (International Association for the Physical Sciences of the Ocean), NIST Standard Reference
86 Material 1640a and 1643e (National Institute of Standards and Technology), and two in-house
87 standards (JUB-1 and CAU Anna Louise black smoker hydrothermal fluids). In-house standards
88 were used for Au, as there are no certified reference data available for this element in seawater.
89 The Au blank was 0.07 ng/kg; nearly 4 orders of magnitude lower than the lowest measured Au
90 concentration in the sampled liquids. This, together with the uniformly high values in all

samples, indicates that gold concentrations measured in the liquids cannot be traced to sampling methodology or laboratory procedures. Data for total Au (dissolved plus particulate) are reported in this study; results for the other trace elements will be reported elsewhere.

AVS/CRS were measured following the sequential method of Fossing and Jørgensen (1989) as presented in Yücel et al. (2011) and Gartman et al. (2014). AVS was distilled under nitrogen flow upon addition of 5 mL HCl (5 M) for 1.5 hours and was trapped as ZnS in 10-15 mL of anoxic zinc acetate (5 % w/v). CRS was then distilled for one hour after injection of 5 mL acidified Cr(II) (1.2 M). The Cr(II) solution was prepared by reducing a Cr(III) solution with zinc metal under nitrogen flow. Sulfide in the traps was quantified using the methylene blue spectroscopic method (Cline, 1969) at 665 nm. The detection limit for this method is 1 μM sulfide.

3. Scanning Electron Microscopy/ Energy Dispersive X-Ray Spectroscopy (SEM/EDS)

Fluid samples were prepared for SEM/EDS by resuspending centrifuged pellets (prepared shipboard) into Milleq® water, then evaporated directly onto 12.5 mm Ted Pella Inc. aluminum stubs. The samples were then rinsed several times with Milleq® water to remove salts, and run on a Tescan VP-SEM in high vacuum mode, without conductive coating. Imaging was performed using both secondary electron and backscatter detectors. Elemental analyses were performed at 20 kV and 14 mm working distance. The detection limit for elemental analysis is 0.1 wt% for a flat sample. Particle dimensions were measured using ImageJ; for Fig. 3, the dimensions for each particle were averaged.

For the chimney sections, mineral identification and trace element composition analyses were performed on raw and epoxy-mounted slabs using a FEI MLA 650F SEM/EDS detector under high vacuum. Images were captured using both electron backscatter and secondary electron imaging. Analysis of slabs was preferred over polished thin sections to avoid the possibility of Au grains being removed during polishing. Slabs were carbon coated prior to analysis. Elemental analyses were performed at 25 kV and a working distance between 13.6 and 15.1 mm. The detection limit for flat samples is 0.1 wt%.

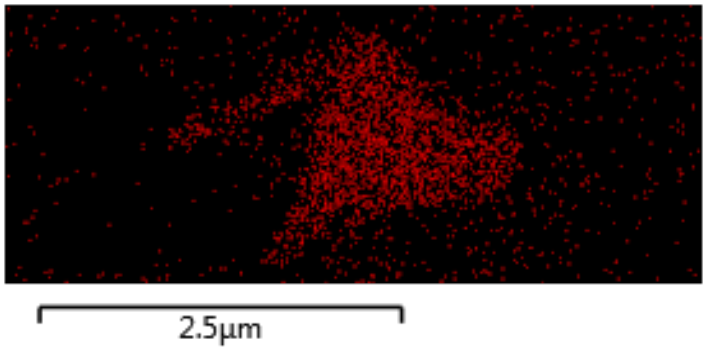
2.5µm


Spectrum 327
Au
O
C
cps/eV
keV

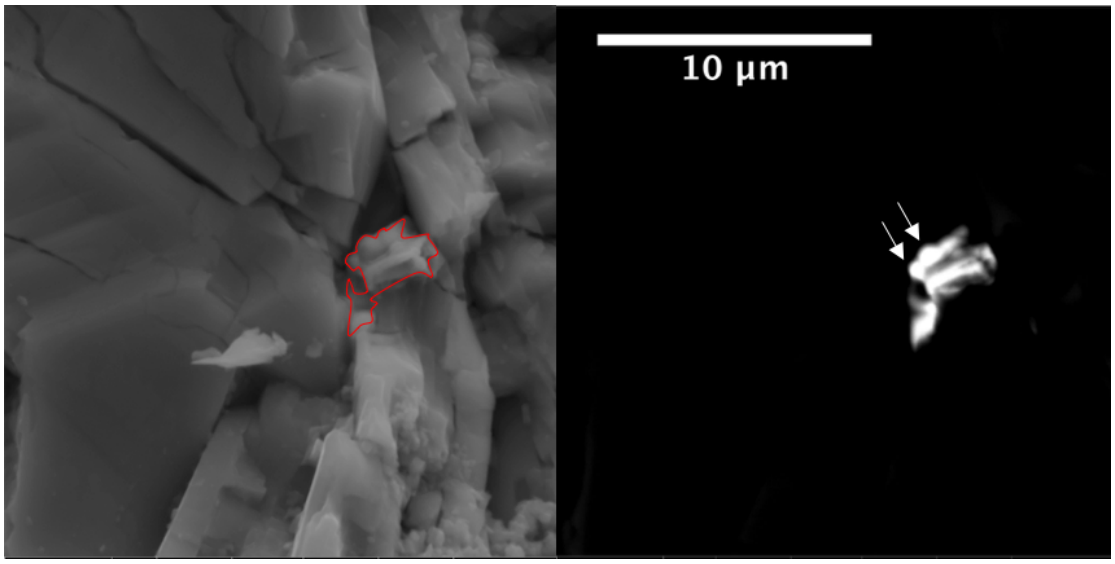
10 µm

Fig. S3- Supporting SEM information. Top to bottom, map of Au Mα for the Au particle shown in Fig. 2B, center, EDS spectra for the same particle, collected at 20 kV, and bottom, secondary electron (left) and backscatter (right) micrograph of a gold particle from the diffuse flow, sulfide chimney; in the secondary electron image, the gold is outlined, and in the backscatter image, the arrows indicate the location of apparent colloids.

4. Chimney Sampling and Analysis

Paired samples of chimney material (mainly lining the orifice of the sampled vents) were collected for mineralogy and bulk geochemistry. Bulk gold concentrations in the chimney samples (Table S1) were determined by instrumental neutron activation analyses (INAA) performed by Activation Laboratories, Ancaster, Ontario.

5. Observed snorkel tarnish and fluid boiling

The pressure and temperature of fluid boiling is plotted after Bischoff, 1991 (Fig. S4). The grey line is the boiling curve from Bischoff,. The red X represents the boiling vent from Niua, given the temperature measured *in situ* and the calculated pressure at the depth of collection, which plots on the boiling curve. The orange +s represent the same parameters for the other samples from Niua. All other samples are cooler than the boiling temperature at the depth of sampling.

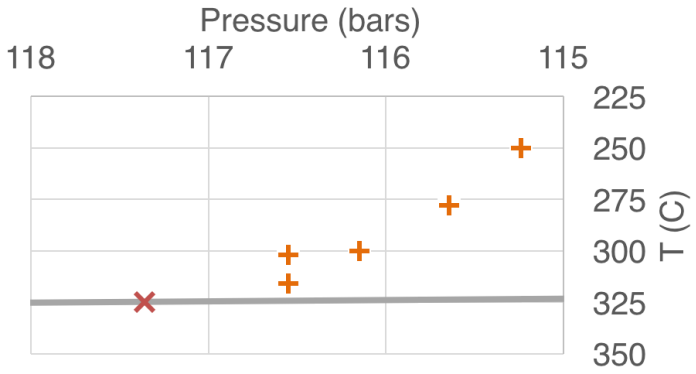

Fig. S4- Boiling curve from Bischoff, 1991 with data from Niua added.

6. Gold Saturation States of Pre-Boiled Liquids

Gold solubility was calculated based on the estimated pre-boiling composition of the vent fluids (T, pH, H_2, and H_2S). pH was assumed to be the measured pH at 25°C plus 1.25 pH unit. H_2 was estimated from the PEQMAP buffer (plagioclase-epidote-quartz-magnetite-anhydrite-pyrite) commonly used for seafloor hydrothermal fluids after Seyfried and Ding (1995) and Seyfried et al. (1999). H_2S concentrations were assumed to be equivalent to the measured AVS+CRS values, although these are minimum values for the pre-boiled fluid, as the samples were collected post-boiling and gases are assumed to be lost upon boiling. Chloride was assumed to be equivalent to preboiled seawater (540 nM). Equilibrium constants were calculated using the HCh software package (Shvarov, 2008). Thermodynamic data for the different aqueous gold species are taken from the compilation of Pokrovski et al. (2014), including the data of Akinfiev and Zotov (2010). Data for other species (e.g., PEQMAP buffer) are taken from most recent version of the SUPCRT92 database (Johnson et al., 1992). The calculated total solubilities for all aqueous species are compared to the measured concentration of Au (including particles) in the sampled fluids in Fig. S3. Except for the low-temperature diffuse vent (250°C), the sampled fluids are all

strongly undersaturated relative to the calculations performed for fluids prior to boiling. Boiling and loss of H_2S must drive the fluid to lower total Au solubility, thus causing precipitation of the Au colloids.

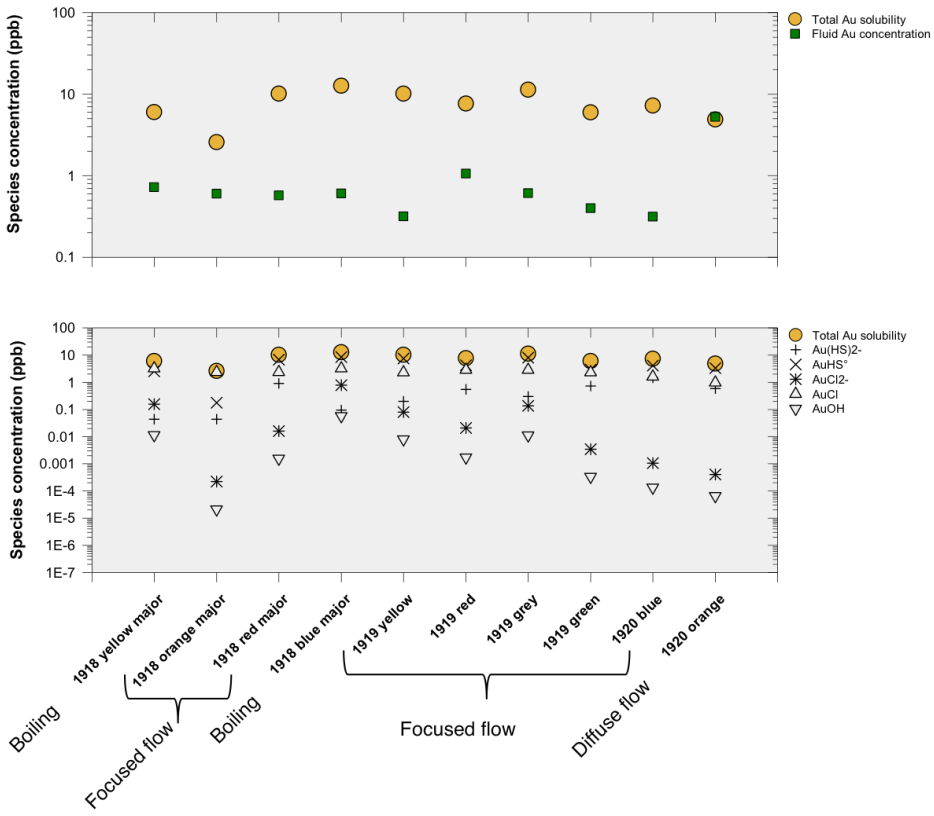

Fig. S5- Calculated solubilities for fluids from Niua, assuming conditions prior to seafloor emission and prior to boiling.

SUPPLEMENTARY REFERENCES

Akinfiev, N.N., and Zotov, A.V., 2010, Thermodynamic description of aqueous species in the system Cu–Ag–Au–S–O–H at temperatures of 0–600C and pressures of 1–3000 bar: Geochemistry International, v. 48, p. 714–720.

Bischoff, J.A., 1991, Densities of liquids and vapors in boiling NaCl-H_2O solutions: A PVTZ summary from 300° to 500°C: American Journal of Science, v. 291, p. 309-338.

Cline, J.D., 1969, Spectrophotometric determination of hydrogen sulfide in natural waters: Limnology and Oceanography, v. 14, no. 3, p. 454-458.

Fossing, H., and Jørgensen, B.B., 1989, Measurement of bacterial sulfate reduction in sediments: Evaluation of a single step chromium reduction method: Biogeochemistry. v. 8, no. 3, p. 205-222.

Garbe-Schönberg, D., 1993, Simultaneous determination of thirty-seven elements in twentyeight international rock standards by ICP-MS: Geostandards Newsletter, v. 17, p. 81–97.

Gartman A., Findlay A. J., and Luther G.W. III., 2014, Nanoparticulate pyrite and other nanoparticles are a widespread component of hydrothermal vent black smoker emissions: Chemical Geology, v. 366, p. 32-41.

Johnson, J. W., Oelkers, E. H., and Helgeson, H. C., 1992, SUPCRT92: A software package for calculating the standard molal thermodynamic properties of minerals, gases, aqueous species, and reactions from 1 to 5000 bar and 0 to 1000°C: Computers & Geosciences, v.18, p. 899–947.

Koschinsky, A., Garbe-Schönberg, D., Sander, S., Schmidt, K., Gennerich, H., and Strauss, H., 2008, Hydrothermal venting at pressure-temperature conditions above the critical point of seawater, 5°S on the Mid-Atlantic Ridge: Geology, v. 36, p. 615–618.

Pokrovski, G.S., Akinfiev, N.N., Borisova, A.Y., Zotov, A.V., and Kouzmanov, K., 2014, Gold speciation and transport in geological fluids: insights from experiments and physical-chemical modelling, in Garofalo, P.S., and Ridley, J.R. (eds) Gold-Transporting

232 Hydrothermal Fluids in the Earth's Crust: Geological Society, London, Special Publication
233 402, p. 9–70.
234 Resing, J., Embley, R., Merlse, S., and Shipboard Scientific Party, 2012, Submarine Ring of Fire-2012
235 (SRoF-12) Northeast Lau Basin: R/V Roger Revelle Expedition RR12111, Cruise Report Sept 9-25,
236 2012, Suva-Samoa, 260 p.
237 Seyfried, W.E. Jr., and Ding, K., 1995, Phase equilibria in subseafloor hydrothermal
238 systems: A review of the role of redox, temperature, pH, and dissolved Cl on the
239 chemistry of hot spring fluids at mid-ocean ridges: Geophysical Monograph Series,
240 vol. 91, pp. 248–272.
241 Seyfried, W.E. Jr., Ding, K., Berndt, M.E., and Chen, X., 1999, Experimental and theoretical
242 controls on the composition of mid-ocean ridge hydrothermal fluids: Reviews in
243 Economic Geology, v. 8, 181–200.
244 Shvarov, Yu.V., 2008, HCh: New potentialities for the thermodynamic simulation of
245 geochemical systems offered by Windows: Geochemistry International, v. 46, p. 834-839.
246 Yücel, M., Gartman, A., Chan, C.S., Luther, G.W., III., 2011, Hydrothermal vents as a
247 kinetically stable source of iron-sulphide-bearing nanoparticles to the ocean: Nature
248 Geoscience, v. 4, p. 367-371.